THE JOURNAL OF COMPARATIVE NEUROLOGY 385:405–414 (1997)

Glycine Immunoreactivity and Receptor Binding in the Cochlear Nucleus of C57BL/6J and CBA/CaJ Mice: Effects of Cochlear Impairment and Aging

JAMES F. WILLOTT,[1]* JOSEPH C. MILBRANDT,[2] LORI SEEGERS BROSS,[1] AND DONALD M. CASPARY[2]

[1]Department of Psychology, Northern Illinois University, DeKalb, Illinois 60115
[2]Department of Pharmacology, Southern Illinois University School of Medicine, Springfield, Illinois 62702

ABSTRACT

Glycinergic neurons in the cochlear nucleus (CN) of C57BL/6J (C57) and CBA/CaJ (CBA) mice were studied by using immunocytochemical and receptor-binding techniques. Adult C57 mice exhibit progressive cochlear pathology as they age, whereas aging CBA mice retain good hearing. In the CN of old C57 mice (18 months) with severe hearing loss, the number of glycine-immunoreactive neurons decreased significantly. The number (B_{max}) of strychnine-sensitive glycine receptors (GlyR) decreased significantly in the dorsal CN of old C57 mice. Significant effects were not observed in the CN of middle-aged C57 mice (with less-severe hearing loss) or in very old CBA mice (which do not exhibit severe hearing loss). The data suggest that the combination of severe hearing loss and old age results in deficits in one or more inhibitory glycinergic circuits in the CN. J. Comp. Neurol. 385:405–414, 1997.

Indexing terms: immunocytochemistry; hearing loss; cochlear nucleus; presbycusis

A growing body of evidence indicates that a diminution of neural inhibition in the inferior colliculus (IC) can accompany aging, and this is likely to involve the inhibitory neurotransmitter γ-aminobutyric acid (GABA; Willott et al., 1988a; Banay-Schwartz et al., 1989; Caspary et al., 1990, 1995; Milbrandt et al., 1994, 1996, 1997; Raza et al., 1994). The occurrence of age-related cochlear pathology also appears to disrupt inhibition in the IC (Willott et al., 1988b; Palombi and Caspary, 1996a,b; Willott, 1996). Age-related changes in neural inhibition in the cochlear nucleus (CN) have been less well studied than those in the IC, but there are indications of age-related effects in CN neurons utilizing glycine, a major inhibitory neurotransmitter in the CN and other nuclei of the lower auditory brainstem (Milbrandt and Caspary, 1995). The present study evaluates the effects of aging and age-related cochlear pathology on glycinergic neurons of the dorsal CN (DCN).

We used two inbred mouse strains to help distinguish between the central effects of cochlear pathology and age-related changes in the brain that occur irrespective of cochlear damage. Progressive age-related cochlear degeneration inevitably occurs in adult C57BL/6J (C57) mice, caused by a gene (*ahl*) on chromosome 10 (Erway et al., 1993; Willott et al., 1995). By 6 months of age, C57 mice exhibit high-frequency hearing loss, which continues to worsen with age; by 18 months of age, they have become severely hearing-impaired (Mikaelian, 1979; Henry and Chole, 1980; Willott, 1986; Hunter and Willott, 1987; Shone et al., 1991; Li, 1992). If progressive cochlear pathology were sufficient to cause changes in glycinergic neurons of the CN, this should be seen in middle-aged C57 mice. By contrast, CBA mice maintain good hearing until late in life (Henry and Chole, 1980; Willott, 1986). If age-related changes were to occur in glycinergic neurons of old CBA mice, it would suggest that biological age effects, independent of cochlear hearing loss, are sufficient to affect glycinergic neurons. Thus, we evaluated glycine immunoreactivity and strychnine-sensitive glycine receptor (GlyR) binding in the CN of young and old mice of these strains.

Grant sponsor: NIH; Grant numbers: R37 AG007554, DC-00151.

*Correspondence to: Dr. James Willott, Department of Psychology, Northern Illinois University, DeKalb, IL 60115. E-mail: jimw@niu.edu

Received 20 September 1996; Revised 4 February 1997; Accepted 26 March 1997

We focus on the two types of glycinergic neurons in the DCN, which have been fairly well characterized, the vertical or tuberculoventral cells and the cartwheel cells. Vertical cells in DCN layer III are activated by branches of auditory nerve fibers and send inhibitory projections to the anteroventral CN (AVCN) and fusiform cells of DCN layer II (Wickesberg et al., 1994). Much evidence indicates that vertical cells are glycinergic (Feng and Vater 1985; Wickesberg and Oertel 1988, 1990; Osen et al. 1990; Saint Marie et al. 1991, 1993; Altschuler et al., 1993; Oertel and Wickesberg, 1993). Cartwheel neurons are located in DCN layer I and the border of layers I and II. Cartwheel neurons appear to immunostain particularly well for glycine but may also stain for GABA; other neurons in the superficial DCN are immunoreactive for GABA only and are likely to represent Golgi or stellate cells (Wenthold et al., 1987; Osen et al., 1990; Saint-Marie et al., 1991, 1993; Wenthold, 1991; Kolston et al., 1992). Cartwheel neurons are innervated by CN granule cells which, in turn, receive input from type II spiral ganglion cells (Brown et al., 1988; Berglund and Brown, 1994) and project to fusiform cells of DCN layer II (Mugnaini, 1985; Berrebi and Mugnaini, 1991; Zhang and Oertel, 1994). Cartwheel neurons also respond to somatosensory stimuli associated with pinnae movements (Young et al., 1995). Input to both vertical and cartwheel neurons should be diminished in aging C57 mice with cochlear degeneration. Because vertical cells receive direct input from primary auditory fibers, they would be directly relieved of their input. Cartwheel neurons would have reduced input from the cochlea (via the granule cells), as well as reduced somatosensory input from the pinnae, because they no longer exhibit startle reflexes or spatial orientation to sounds (Parham and Willott, 1988).

MATERIALS AND METHODS

Glycine immunocytochemistry

Subjects. C57 and CBA mice of either sex were obtained from our own mouse colony. They were first- to third-generation offspring of stock procured from Jackson Laboratory (Bar Harbor, ME). After weaning, the animals were separated into same-sex cohort groups, raised in wire mesh cages, and given free access to tap water and Purina Rodent Chow (Ralston-Purina, St. Louis, MO). The room temperature was maintained between 23° and 24°C and a 12-hour light-dark schedule was used, with light onset at 7:00 a.m.

C57 mice of the following age groups were used: 1-month-old (mean age 33.4 days; range 28–54 days, n = 10), 12-month-old (aged 11–12 months, n = 6), 18-month-old (n = 4), and 29 months (aged 28–30 months, n = 4). CBA mice included 2-month-old (n = 3), 12-month-old (n = 2), and 37 months (aged 36–38 months, n = 4).

Tissue preparation

Perfusion/fixation. Animals were anesthetized deeply with Nembutal and intracardially exsanguinated with 0.05% sodium nitrite in physiological saline, followed by a 20-minute perfusion with fixative containing 1% paraformaldehyde and 1.25% glutaraldehyde in 0.1 M phosphate buffer, pH 7.4.

Preparation of tissue. Each brain was removed from the skull and placed in fixative for another 2–4 hours, stored overnight at 4°C in 5 mM phosphate buffered saline (PBS), and then sectioned frontally at 50 µm by using a Vibratome (Technical Products International, St. Louis, MO). Following rinses in PBS, sections were preincubated in a blocking solution of 3% normal goat serum (NGS) in PBS with 0.3% Triton X-100 and then incubated in a primary antibody solution for 18–24 hrs at 4°C. The primary antibody solution contained affinity-purified, polyclonal rabbit antisera diluted in 3% NGS in PBS as follows: anti-glycine (Biogenesis, Inc., Franklin, MA) diluted 1:500–1:1,000, and anti-GABA (Sigma, St. Louis, MO) diluted 1:2,000–1:2,500. Alternate serial sections from the same brain were incubated in different antibody solutions (with the exception of DCN layer I, the data on GABA immunoreactivity are not presented in this study). Control sections were incubated in the blocking solution diluent to which no primary antibody was added. After rinsing in PBS, visualization of the primary antibody was achieved via an avidin-biotin-peroxidase technique using the Vectastain ABC kit (Vector Labs, Burlingame, CA) and, following rinses, subsequent treatment with peroxidase substrate prepared from SIGMA FAST DAB (3,3′-diaminobenzidine) peroxidase substrate tablet sets (Sigma). Finally, the sections were washed with dH_2O, mounted on subbed slides, allowed to dry overnight, and then coverslipped with either Pro-Texx or Accu-Mount 280 (Baxter, McGaw Park, IL) mounting media.

Quantitative analysis of immunostained sections. Images were captured from a Nikon Microphot-FX light microscope (Nikon, Garden City, NY), mounted with a Javelin Ultrichip high-resolution video camera (Javelin, Los Angeles, CA) by using a Targa+ frame grabber board (Truevision, Indianapolis, IN). Captured images were analyzed by using either JAVA or Mocha (Jandel Scientific, San Rafael, CA) image analysis software. The image analysis system was used to establish an objective criterion for acceptance of a neuron as immunoreactive, measuring cells whose gray-scale intensity levels fell within a defined range. Virtually all glycinergic cells in the medial nucleus of the trapezoid body medial nucleus of the trapezoid body (MNTB) would fall within this range, whereas cells that appeared lightly stained, but were known not to be glycinergic, would not. The range was set without knowledge of the subject's age and was held constant for each individual. The area of the tissue measured was also determined by Mocha. Neuron density was computed by totaling the cell count data and the area measured and calculating one density for each animal. As a reliability check, some tissue sections were also evaluated by a 'blind' observer using an eyepiece reticle and subjective judgment of immunoreactive neurons. The relative differences in densities between subject groups were very similar for both methods of evaluation.

For evaluation of the number of immunoreactive cells, an attempt was made to examine comparable sections for each animal. In DCN layer III (the location of vertical cells), a posterior and anterior DCN section was chosen for each animal; sections were examined from every subject. This was a sufficient sample because the rostrocaudal dimension of DCN layer III is approximately 500 µm (ten 50-µm sections), and the distribution of glycine-immunoreactive neurons is rather uniform (see Wickesberg et al., 1994). For immunoreactive cells in the superficial DCN (layer I and the border between layers I and II; presumably cartwheel neurons), three standard sections were evaluated for each mouse. Because some neurons in this region are also immunoreactive for GABA (Wenthold et al., 1987; Wenthold, 1991; Kolston et al., 1992), neurons

labeled for GABA antibody were evaluated as well. For the AVCN, the region anterior to the auditory nerve root was examined, and counts were performed on scattered small cells that were very darkly stained. Because of some technical difficulties, AVCN data were not available on all subjects (C57s: 1 month n = 6; 12 month n = 2; 18 month n = 2; 29 month n = 4. CBAs: 2 month n = 0, 37 month n = 3). It was not possible to examine standard sections for the large 'commissural' neurons around the auditory nerve root, because these were more scattered in the anterior-posterior dimension and a border could not be determined for a specific area of CN. Thus, three to five sections containing auditory nerve root were examined, and the number of cells per section was determined. For the MNTB, all glycine-positive cells were counted for the section in which the MNTB appeared to have the largest cross-sectional area.

Packing density of immunoreactive cells. The packing densities are presented with the number of immunoreactive cells at one plane of focus per area of the structure in that tissue section. The plane of focus was that in which the greatest number of immunoreactive neurons could be seen. The critical data for the present study are the relative comparisons of packing densities across subject groups.

Density corrected for age-related changes in the size of CN subdivisions. Age-related changes in the dimensions of a CN subdivision can influence the packing density and provide misleading data about the overall number of immunoreactive neurons as a function of age group (e.g., if density increases but the CN volume decreases, the total number of neurons could remain the same). Thus, packing densities were 'adjusted' for changes in the size of the AVCN, DCN, and MNTB. The tissue sections prepared for immunocytochemistry are not well suited for accurate determination of CN subnucleus dimensions, so age-related changes established by earlier studies of the C57 and CBA CN (Willott et al., 1987, 1992) were used for the adjustments (an attempt was made to corroborate previous age-related changes with the present material as well). In contrast to the CN, the MNTB can be clearly delineated by the glycine immunoreactivity of its neurons, and the present material was used to compare the size of the MNTB across age groups to adjust the densities (such data have not been obtained by any previous studies).

The adjusted packing densities should more accurately reflect age-related differences in the total number of immunoreactive neurons across subject groups. For each age group, the age-related changes in the size of the structure (DCN layer III, MNTB, etc.) were expressed as a percent difference with 1-month-old mice of the same strain. The packing density was then multiplied by that fraction to adjust for age-related differences in volume.

Potential for sampling bias. The potential for sampling bias (see Saper, 1996) should be minimal in this study. First, as discussed earlier, adjustments were made to correct for the effects of age differences in subnucleus size on packing density. Second, age-related changes in the size of CN neurons are not great in these mouse strains (Willott et al., 1987, 1992), so that sampling bias based on neuron size should not be a factor. Third, earlier morphological studies of the mouse CN, utilizing observations in all three cardinal planes (Willott et al., 1992), indicate that the packing density is fairly uniform throughout any particular CN subdivision. Our unpublished observations and those of others (Wickesberg et al., 1994) indicate that this is true about the packing density of glycine-immunoreactive neurons in the mouse CN as well. Thus, the packing density of any section within a CN subnucleus should be representative. Fourth, by examining immunostaining in the MNTB, we eliminated the likelihood that differences in immunoreactivity as a result of aging per se would produce sampling bias. All of these considerations indicate that the data analysis, which focuses on relative differences in adjusted packing densities across age groups, should not be subject to sampling bias.

Statistical analysis of immunocytochemistry. Packing densities of immunoreactive neurons were compared across age groups by using one-way analysis of variance (ANOVA) for each structure ($\alpha = 0.05$). Separate analyses were performed for C57 and CBA mice because the age groups were not identical for each strain. Significant ANOVAs were followed by Tukey tests ($\alpha = 0.05$) to compare individual age groups.

Glycine receptor binding

Subjects. For the receptor binding studies, age groups were 'young adults' (1.5- and 3-month-olds), 'middle-aged' (7- and 12-month-olds), and 'old' (24- to 27-month-olds). For DCN experiments, the number of subjects in each age group was 9, 11, and 10 (C57 mice) and 6, 6, and 6 (CBA mice), respectively. For AVCN experiments, the number of subjects in each group was 6, 6, and 6 (C57 mice) and 5, 5, and 8 (CBA mice), respectively.

Tissue preparation. The mice were decapitated, and the brains were rapidly removed and frozen in dry ice. The brains were allowed to equilibrate in a cryostat (Minotome, International Equipment Company) at −20° to −15°C, and serial transverse sections (20 μm) were collected from the center of the rostral-caudal extent of the AVCN and from the DCN. Frozen sections were warm-mounted on chrome-alum/gelatin-coated slides and stored at −20°C for a time not exceeding 48 hours. Location within the AVCN and the DCN was verified by counterstaining adjacent sections.

Autoradiography to detect ligand binding. Strychnine binding sites were examined by using a modified protocol of Zarbin and colleagues (Zarbin et al., 1981). Tissue sections were subjected to two 25-minute prewashes in 50 mM Na^+-K^+ phosphate buffer (pH 7.4 at 4°C) and dried under cool air. Slides were incubated for 20 minutes in 50 mM Na^+-K^+ phosphate buffer (pH 7.4 at room temperature) containing 2–32 nM [^{3}H]strychnine (22–26 Ci/mmol, New England Nuclear, Boston, MA). Nonspecific binding was determined in adjacent sections by the addition of 10.0 mM glycine to the ligand buffer. Incubation was terminated by a quick dip in 50 mM Na^+-K^+ phosphate buffer (pH 7.4 at 4°C), a 2-minute wash in fresh 50 mM Na^+-K^+ phosphate buffer (pH 7.4 at 4°C), one quick dip in deionized water at 4°C, and then the sections were dried under warm air. A 2-minute final wash was chosen on the basis of previous studies showing the removal of a substantial amount of nonspecific binding while retaining a very large percentage of total binding (Zarbin et al., 1981).

Autoradiograms were generated by apposing the slides and a commercial standard containing known amounts of radioactivity to ^{3}H-sensitive film (Amersham, Hyperfilm-^{3}H). Following a 4- to 5-week exposure time at 4°C, the films were developed in Kodak D19 (Eastman-Kodak,

Rochester, NY) for 4 minutes at room temperature, stopped in 1% acetic acid, fixed in Kodak rapid fixer, washed, and air dried.

Quantitation and data analysis. Ligand binding was quantified by using computer-assisted densitometry software (MCID, St. Catherines, Ontario, Canada). Films were placed on a light box, and digitized images were captured by using a CCD video camera. Average optical density was determined by taking multiple density readings from the area of interest. A standard curve was generated from coexposed ^{14}C-embedded plastic standards (ARC, St. Louis, MO). These commercial standards have been previously calibrated against known amounts of tritium and protein (Pan et al., 1983). Use of these standards allows for the conversion of areal optical density to fmol/mg protein. Saturation data were determined by using a Scatchard analysis. K_d and B_{max} values were determined for each animal, and these data were combined to determine means and standard deviations (normalized re: young mice) for each age group. Statistical differences between age groups were determined by ANOVA (one-way analysis of variance, Tukey follow-up test).

All animal protocols for the care and use of animals were approved by the Institutional Animal Care and Use Committee of Northern Illinois University and are in conformance with NIH guidelines.

RESULTS

Glycine immunocytochemistry

Four types of glycine-immunoreactive neurons were readily visible, irrespective of age or strain. These include medium-sized neurons in DCN layer III, presumed to be vertical (tuberculoventral) neurons; medium-sized neurons in DCN layer I and II, presumed to be cartwheel neurons); small, darkly stained neurons in the AVCN; and large neurons in and around the auditory nerve root, presumed to be commissural neurons (Schwartz, 1981; Caspary et al., 1985; Altschuler et al., 1986; Wu and Oertel, 1986; Wenthold 1987; Wenthold et al., 1987; Kolston et al., 1992; Zhang and Oertel, 1993; Wickesberg et al., 1994).

Immunoreactive cells in the DCN layer III. Figure 1C shows a typical example of a section in the DCN of 1-month-old C57 in which immunoreactive cells are plentiful in DCN layer III. By contrast, in 29-month-old C57 mice, glycine-positive cells were virtually absent (Fig. 1D). The quantitative analysis supports these observations. For C57 mice (Fig. 2, filled circles), the volume-adjusted packing density of immunoreactive neurons in DCN layer III (presumably vertical cells) changed little between 1 and 12 months of age and then began to decrease [$F(3,18) = 7.90$, $P = 0.0014$]. Tukey tests showed that the packing density in 29-month-old mice was significantly lower than that of 1-, 12- and 18-month-old mice. [The adjustments in density for the above data used volumetric values from Willott et al. (1992) to obtain the following multipliers: 1-month-olds: 1.0; 12-month-olds: 0.86; 18-month-olds: 0.82 (interpolated from data on 12-and 24-month-olds); 29-month-olds: 0.66 (note that the volume changes estimated from our present immunocytochemical material are similar to what was found in the Willott et al. (1992) study: with respect to young mice, 0.90 for 12 month-olds; 0.67 for 29-month-olds).]

For CBA mice, packing densities of immunoreactive cells did not differ significantly as a function of age [$F(2,6) = 0.084$, $P = 0.92$], as seen in Figure 2 (unfilled circles). [Densities did not need to be adjusted for volume changes because neither the earlier study on 29-month-old CBA mice (Willott et al., 1992) nor our observations on the present material (which extended the ages to 37 months) indicated a significant difference in the size of DCN layer III as a function of age.]

Comparisons between strains. Packing densities of glycine-positive neurons did not differ between 1-month-old C57 and 2-month-old CBA mice [$F(1,11) = 0.00033$, $P = 0.986$], indicating that young adult mice of each strain were very similar in this respect. However, the packing density of 29-month-old C57 was significantly lower than that of 37-month-old CBA mice [$F(1,6) = 37.26$, $P = 0.0009$].

Immunoreactive cells in DCN layer I. It can be seen in Figure 1C that, as was the case for DCN layer III, immunoreactive neurons were present in layer I of young C57 mice but declined in old mice (Fig. 1D). For C57 mice (Fig. 2, filled diamonds), the relative density of glycine-immunoreactive neurons in DCN layer I and bordering layer II (presumed to be cartwheel neurons) exhibited an age-related change similar to that observed for neurons in layer III, with a decline observed during the second year of life. The age effect was significant [$F(3,16) = 9.08$, $P = 0.001$], with Tukey tests indicating that the density of the 29-month-old group was significantly less than that of the other three age groups. [The volume of DCN layer I is significantly reduced only in 29-month-old C57 mice (Willott et al., 1992), by a factor of 0.69, and this value was used to adjust the density in the above analysis.]

Because some neurons in DCN layer I (and near the border of layer II) are immunoreactive for both glycine and GABA antibodies (Kolston et al., 1992), the age difference between 1- and 29-month-old C57 mice was also examined with respect to the number of neurons labeled for GABA antibody. Although the adjusted density of glycine-positive neurons decreased by 61% from 1 to 29 months (see Fig. 2), the adjusted density of GABA-positive neurons decreased by only 27%. A two-way ANOVA (Age by Antibody) yielded

Fig. 1. Immunoreactive neurons in young and old C57 mice. For orientation, all are frontal sections. **A:** Nissl-stained section of the dorsal cochlear nucleus (DCN) of a young C57 mouse. The three DCN layers are numbered; arrows indicate the borders between the layers (I/II; II/III; III/DCN border). **B:** Control section incubated in the blocking solution diluent to which no primary antibody was added. **C:** Glycine immunostaining typical of the DCN of a 1-month-old C57 mouse. Immunoreactive neurons are seen in DCN layers I–III. Arrows indicate the borders between the layers I/II, II/III, and III/DCN border (see A). **D:** Glycine immunostaining typical of the DCN of a 29-month-old C57 mouse. There is a virtual absence of immunostaining (the highest antibody concentration, 1:500, was used for this section). Arrows indicate the borders between DCN layers in (C) and (D) (see A). **E:** GABA immunostaining typical of the DCN of a 1-month-old C57 mouse. Labeled neurons are seen in layer I/II. Arrow indicates the border between layers I and II (see A). **F:** GABA immunostaining typical of the DCN of a 29-month-old C57 mouse. Labeled neurons are seen in layer I/II in numbers similar to those seen in young mice (E). Arrow indicates the border between the layers I and II (E,F; see A). **G:** Glycine immunostaining in the MNTB typical of a 1-month-old C57 mouse. **H:** Glycine immunostaining in the MNTB typical of a 29-month-old C57 mouse, similar to that seen in young mice (G). Original magnification for all sections = ×200. Scale bar = 100 μm in A–H.

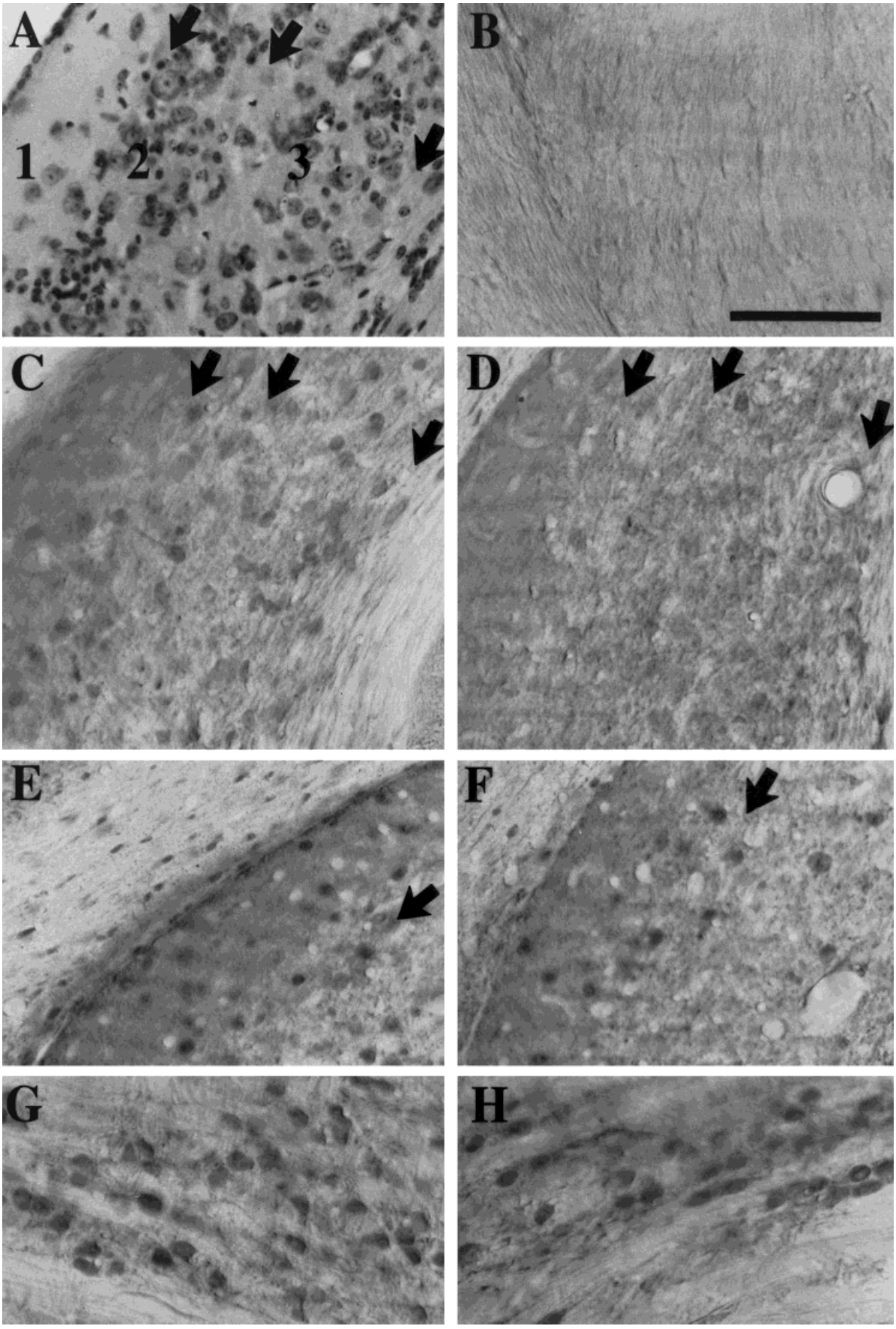

Figure 1

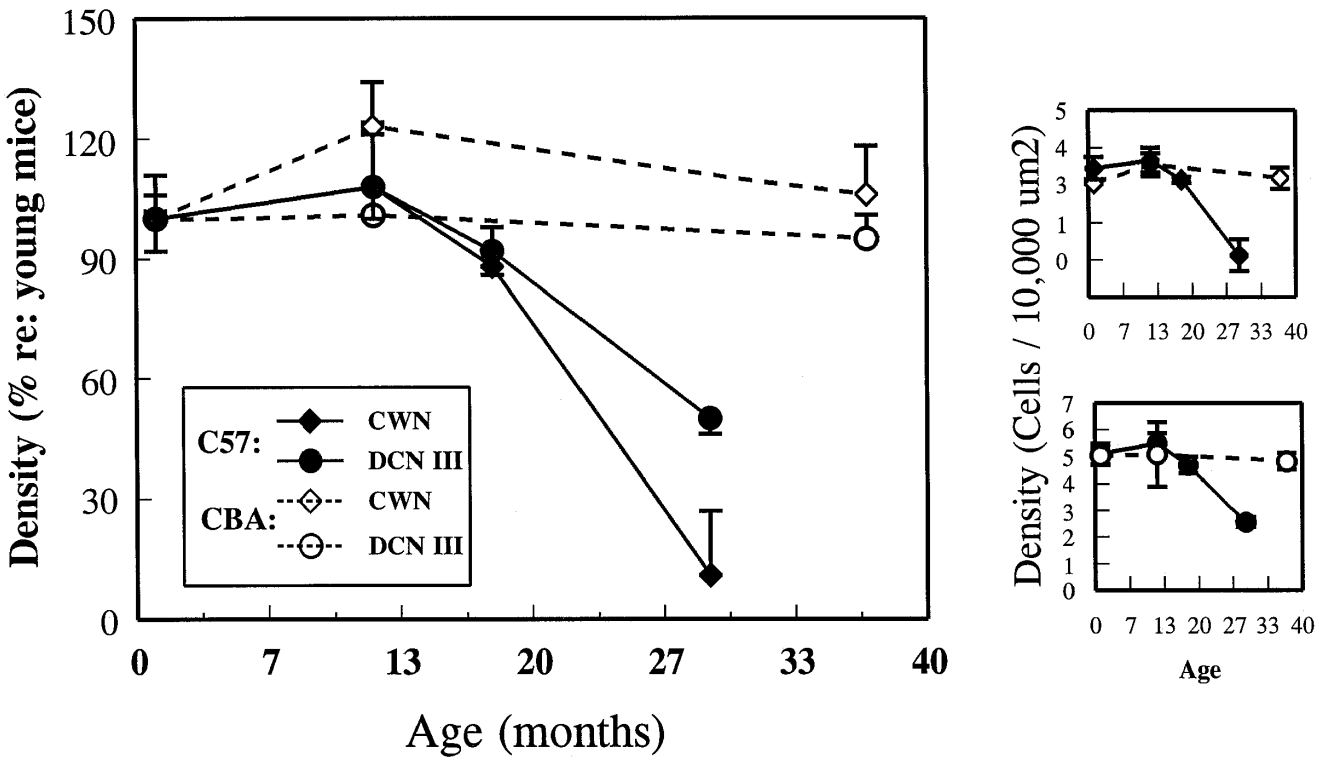

Fig. 2. Density of glycine-immunoreactive DCN neurons in C57 and CBA mice. Left: Shows the relative changes in packing density of glycine-positive neurons as a function of age, where 100% = the density in 1-month-olds. Right: Shows the absolute values of the packing densities. Density values are adjusted for age-related changes in the volume of each structure, as indicated in the text. Error bars = SEM.

significant main effects for both Age (young vs. old) [$F(1,18) = 28.4$, $P < 0.0001$] and Antibody (glycine vs. GABA) [$F(1,18) = 20.9$, $P = 0.0002$]. More importantly, the Age X Antibody interaction was also significant [$F(1,18) = 4.55$, $P = 0.047$]. The age-related decline in glycine-immunoreactive neurons of C57 mice was significantly greater than that of GABA-immunoreactive neurons. This finding is evident in Figure 1E and F, which presents micrographs from sections immunostained for GABA. Numerous cells are immunoreactive for GABA in the old mouse, despite the absence of immunostaining for glycine (compare Fig. 1D and F). If it is assumed that neurons labeled for glycine are cartwheel neurons, whereas those labeled well for GABA but not for glycine are of some other type (Kolston et al., 1992), the data suggest that cartwheel neurons are no longer immunoreactive in aging C57 mice, whereas GABA immunoreactivity (probably being expressed by Golgi or stellate cells) is less affected.

In CBA mice, a significant age effect was not observed for density of DCN layer I cells (Fig. 2, unfilled triangles). For young mice the mean density in DCN layer I was 2.66 cells per 100,000 μm^2, compared with 2.83 cells per 100,000 μm^2 in 37-month-old mice. An age-related change in the thickness of layer I was not apparent in the present tissue, and our earlier study revealed only a nonsignificant reduction in volume for 29-month-old CBA mice compared with young mice (Willott et al., 1992). Thus, neither the packing density of glycine-immunoreactive cells nor volume of DCN layer I appear to be significantly altered with age in CBA mice.

Other immunoreactive cells in the CN. Scattered glycine-immunoreactive neurons were observed in the AVCN. The quantitative analysis showed that for C57 mice, glycine-positive neurons in the AVCN exhibited a decline in packing density from 1.34 cells per 100,000 μm^2 in 1-month-olds to 0.21 cells per 100,000 μm^2 in 29 month-olds [$F(3,10) = 8.324$, $P = 0.0045$; Tukey tests: 29-month-olds differed from each other group]. [Adjustments of density for the above analysis were made on the basis of volumetric data from (Willott et al., 1987), resulting in the following multipliers: 1-month-olds: 1.0; 12-month-olds: 0.95; 18-month-olds: 0.95; 29-month-olds: 0.74.]

As indicated earlier, technical difficulties prevented AVCN analysis of 2-month-old CBA mice. However, 37-month-old CBA mice had a higher density of glycine immunoreactive cells (0.97 cells per 100,000 μm^2) than did 29-month-old C57 mice (0.21 cells per 100,000 μm^2), and this difference was significant [$F(1,5) = 8.81$, $P = 0.031$]. The density of immunoreactive cells in the old CBA mice was similar to that in 1- and 18-month-old C57 mice, suggesting that there was little decline in immunoreactivity in the old CBA mice.

As indicated earlier, it was not possible to delineate a specific area containing immunoreactive neurons around the auditory nerve root (presumed to be commissural neurons), so a quantitative, volume-adjusted analysis of density was not performed. The mean number of immunoreactive neurons (plus standard error) observed in histological sections containing the auditory nerve root were for C57 mice: 1-month-olds: 6.1 (0.88); 12-month-old 8.6 (0.78);

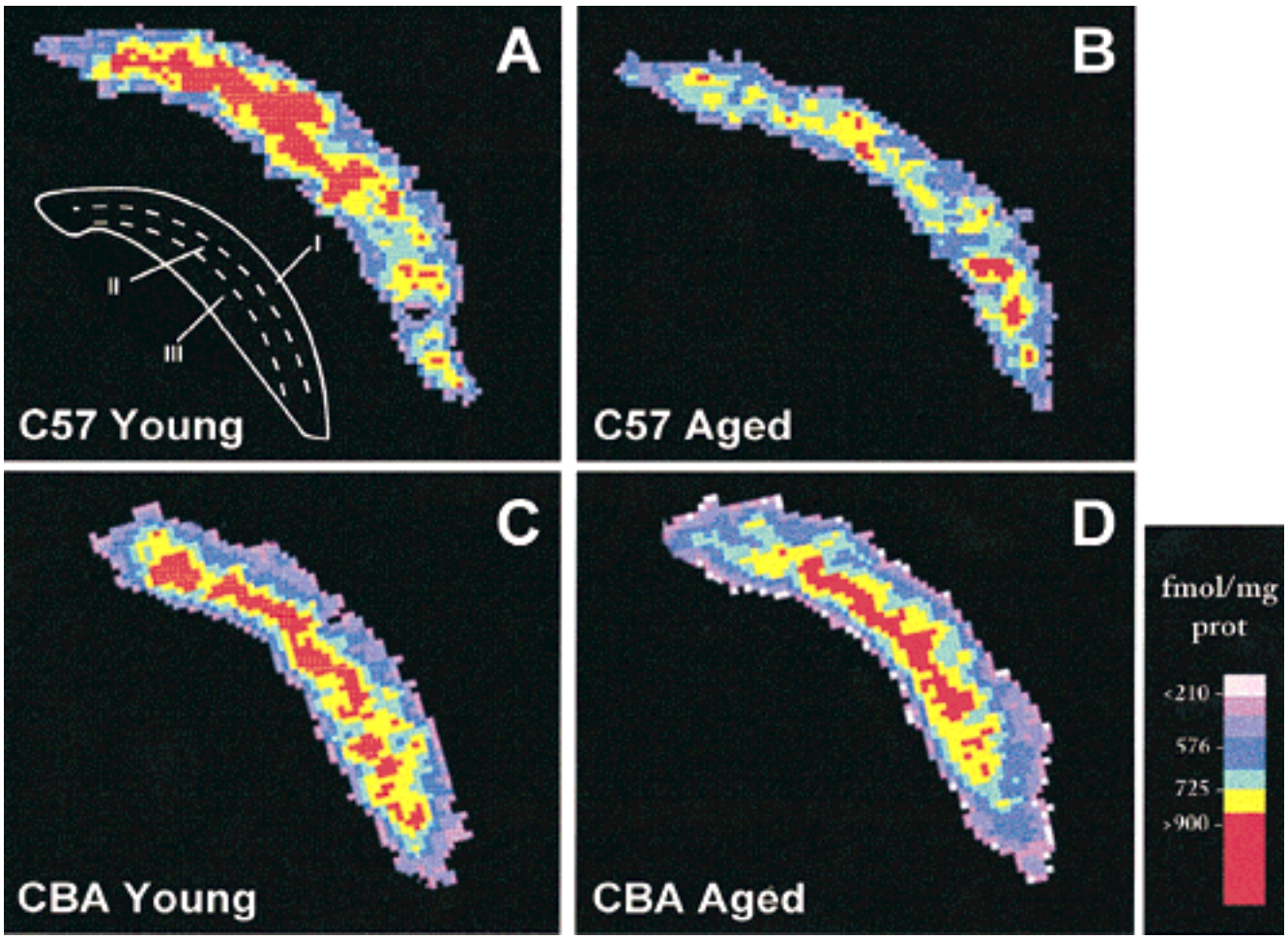

Fig. 3. Color-enhanced digitized images showing strychnine binding in representative C57 (**A**,**B**) and CBA (**C**,**D**) mice. Notice the decrease in binding in the DCN of a 24-month-old C57 mouse (B) when compared with a young adult (3 months old; A). The change appears to be particularly pronounced in DCN layer II (graphic, A), presumably the fusiform cells. In contrast to C57 mice, binding in the DCN of an old (27 months) CBA mouse (D) was not reduced compared with that of a 3-month-old CBA mouse (C). Color scale represents concentration of bound ligand (fmol/mg protein). Roman numerals indicate DCN layers. Scale bar = 0.5 μm.

18-month-olds: 7.7 (1.65); 29-month-olds: 4.8 (0.81). Thus, there appear to be fewer commissural neurons in the 29-month-old C57 mice, although the decline may not be as great as it was for the other CN cell types. The 37-month-old CBA mice were similar to the younger C57 mice, with a mean of 7.0 (0.85) neurons per histological section.

Immunoreactive cells in the MNTB. As a within-subject and within-age group control for immunostaining, glycine-positive neurons in the MNTB were also examined. In old mice C57 mice, immunostaining of MNTB neurons was quite pronounced, as it was for 1-month-olds (compare Fig. 1G and H). There was no age-related decrease in the packing density of glycine-positive MNTB neurons (indeed, the best labeling was observed in 18-month-old C57 mice).

Glycine receptor binding

In both C57 and CBA mice, high levels of binding were observed in the DCN and AVCN. Scatchard analysis obtained from saturation data in the DCN of young adult mice (1.5–3 months) revealed a $K_d = 13.33 \pm 1.6$ nM and $B_{max} = 790.4 \pm 128$ fmol/mg protein for C57 mice and a $K_d = 10.9 \pm 2.8$ nM and $B_{max} = 606 \pm 153$ fmol/mg protein for CBA mice. In the AVCN of young adults, $K_d = 9.23 \pm 2.04$ nM and $B_{max} = 653.7 \pm 35$ fmol/mg protein for C57 mice, and $K_d = 15.2 \pm 5.28$ nM and $B_{max} = 876.9 \pm 115$ fmol/mg protein for CBA mice. There were no significant *between*-strain differences in any measure in young mice. Furthermore, there was no indication of any differences in B_{max} or K_d for 1.5- and 3 month-olds *within* either strain (i.e., no developmental effects between 1.5 and 3 months). Substantial levels of binding were observed in other brainstem nuclei, including the facial nucleus, spinal trigeminal nuclei, and the vestibular nuclei (data not shown). No apparent specific binding was observed in the cerebellum.

Strychnine binding in the cochlear nucleus of older mice. Figure 3 shows color-enhanced digitized images with strychnine binding in the DCN of representative C57 (A and B) and CBA (C and D) mice. Notice the decrease in

binding in the DCN of a 24-month-old C57 mouse (B) compared with a young adult (3 months old, A). The change appears to be particularly pronounced in the vicinity of DCN layer II, presumably the fusiform cells. In contrast to C57 mice, strychnine binding in the DCN of an old (27 months) CBA mouse (D) was not reduced compared with that of a 3-month-old CBA mouse (C). The color scale represents concentration of bound ligand (fmol/mg protein).

GlyR binding (B_{max}). Saturation analysis in the DCN using [^{3}H]strychnine showed the relationship between age and B_{max} values to be consistent with the individual examples depicted in Figure 3. For the DCN of C57 mice (Fig. 4), B_{max} decreased significantly with age in the DCN [$F(2,27) = 4.27$, $P = 0.025$]. Tukey tests showed that B_{max} of the old mice was significantly smaller than that of young adult and middle-aged mice. For the DCN of CBA mice, however, the age effect was not significant, although B_{max} values increased slightly with age (re: young adults: +26% in middle-aged; +37% in old). These data indicate that receptor binding declined in the DCN of old, hearing-impaired C57 mice, but not in aging CBA mice.

The minimal age-related decline of B_{max} in the AVCN of C57 mice (Fig. 4, open circles) was not statistically significant. Similarly, B_{max} did not differ significantly as a function of age in CBA mice (re: young adults: −16% in middle-aged; +15% in old).

GlyR affinity (K_d). In C57 mice K_d decreased by 24% between the ages of 1.5 and 24 months; however, the overall age effect was not statistically significant [$F(2,27) = 2.28$, $P = 0.12$]. No evidence of systematic age-related differences in K_d was observed for the AVCN of C57 mice. For CBA mice the ANOVAs were not significant for the DCN or AVCN, although increases in the old mice were suggested for both DCN (re: young adults: +13% in middle-aged; +79% in old) and AVCN (re: young adults: −39% in middle-aged; +52% in old). Taken together, the data may be viewed as suggestive of a decline in receptor affinity in the DCN of old C57 mice, particularly when contrasted to the increase in old CBAs.

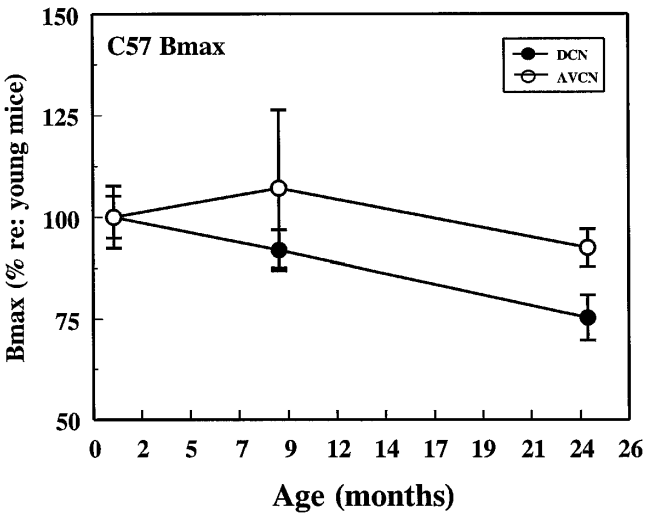

Fig. 4. Normalized data for strychnine binding in the DCN and AVCN of C57 mice. Error bars = SEM.

DISCUSSION

The findings of the present study indicate that neither cochlear pathology prior to old age (12-month-old C57 mice) nor extreme age in the absence of severe cochlear pathology (CBA mice) resulted in significant changes in glycine immunolabeling or GlyR binding. However, the combination of severe hearing loss and age, as occurs in old C57 mice, was accompanied by substantial decline in measures of glycinergic function.

A decrease in the number of glycine-immunoreactive neurons was observed in aging C57 mice only when hearing loss was chronic and severe. This finding could reflect the attrition of glycinergic neurons and/or a loss of immunoreactivity of surviving cells. In our earlier morphological studies of the C57 CN, a significant age-related loss of neurons was observed in DCN layer III (Willott et al., 1992) and the AVCN (Willott et al., 1987); the present data suggest that glycinergic neurons may have been among those that disappeared. On the other hand, no net loss of neurons was observed in either layers I or II of very old C57 mice, suggesting that the cartwheel neurons are still present but no longer exhibit immunoreactivity for glycine. In any event, it is clear that substantially fewer normally glycine-immunoreactive CN neurons are present in old, hearing-impaired C57 mice.

The immunocytochemical findings are nicely complemented by the GlyR binding data. GlyR binding (B_{max}) was significantly reduced in the DCN of old C57 mice, and this decrease was especially evident in DCN layer II (Fig. 3). Vertical cells and cartwheel neurons project to fusiform cells of DCN layer II (see above), so the observed loss of GlyR binding would be expected to accompany the substantial loss or impairment of vertical and cartwheel cells seen in old C57 mice. As discussed earlier, vertical cells also project to the AVCN, which showed little loss of GlyR binding. However, the AVCN also receives significant glycinergic input from the superior olivary complex (Godfrey et al. 1978; Caspary et al. 1979, 1993; 1994; Caspary 1986; Shore et al., 1991; Altschuler et al., 1993; Potashner et al. 1993), which might mask the effects of decreased vertical cell input. The GlyR affinity (K_d) data are less clear, but a nonsignificant decrease in old C57 mice suggests that some age-related changes in receptor affinity may have occurred in the DCN.

The time course for the loss of glycine immunolabeling and GlyR binding observed in the present study lagged well behind the appearance of behavioral and physiological changes repeatedly found in hearing-impaired, middle-aged C57 mice. Behavioral and physiological changes in C57 mice are quite pronounced by 6 months of age (Mikaelian, 1979; Henry and Chole, 1980; Willott, 1986; Hunter and Willott, 1987; Willott and Carlson, 1995), but the declines in glycinergic neurons and GlyR binding did not appear until the second year of life. This temporal disparity does not necessarily rule out functional consequences of impaired glycinergic systems in the CN prior to old age. It is possible that the denervation of the CN neurons must be severe and/or chronic to affect the glycinergic neurons to the extent that they either degenerate or are no longer immunoreactive. Thus, the loss of auditory input could affect inhibitory neurons during the first year of life (contributing to the behavioral and physiological changes), but the present methods may not detect the early effects of denervation.

A good deal of evidence indicates that the attenuation or removal of cochlear input to the CN results in pronounced transneuronal changes in immature animals and substantially less impact on the CN of mature animals (see Willott et al., 1994 for references). The absence of significant immunocytochemical or receptor binding changes in middle-aged C57 mice with hearing loss supports the latter view. However, the findings from old C57 mice suggest that a prolonged period of cochlear pathology (perhaps in combination with other concomitants of aging) can result in dramatic *but selective* changes in the adult auditory system. Glycinergic circuits in the CN appear to be particularly vulnerable, whereas MNTB neurons retain normal immunolabeling for glycine. Furthermore, GABA immunolabeling in the superficial DCN is not greatly diminished. A variety of intracellular events have been implicated in transneuronal denervation effects in young animals (e.g., Lachica et al., 1996), but it is presently unclear what mechanisms are involved here.

Implications for hearing

The present findings indicate that inhibitory glycinergic circuits in the CN are affected in old, hearing-impaired C57 mice, but similar changes do not occur in middle-aged C57 mice with less severe hearing loss or in very old, well-hearing CBA mice. The implication is that old individuals with severe hearing loss are at risk for disruption of inhibitory glycinergic circuits in the CN. Given the vital role glycinergic inhibition plays in CN physiology (e.g., Caspary et al., 1985, 1987, 1993;; Wenthold, 1991; Altschuler et al., 1993; Oertel and Wickesberg, 1993; Saint Marie et al., 1993; Winer et al., 1995), the occurrence of such effects would have important gerontological implications; millions of elderly individuals exhibit cochlear damage, often accompanied by auditory perceptual problems whose cause seems to involve a disruption of normal central processes (Willott, 1991). Thus, it seems important to further elucidate the relationship between hearing loss, inhibitory circuits in the cochlear nucleus, and auditory perceptual problems.

ACKNOWLEDGMENTS

We thank Dr. Robert Helfert for his expert help with the immunocytochemistry and Tina Schanklin and Tracy Schatteman for technical assistance. We also thank Dr. Donata Oertel for helpful comments on an earlier version of the manuscript. This study was supported by NIH grants R37 AG007554 to J.F.W. and DC-00151 to D.M.C.

LITERATURE CITED

Altschuler, R.A., H. Betz, M.H. Parakkal, K.A. Reeks, and R.J. Wenthold (1986) Identification of glycinergic synapses in the cochlear nuclei through immunocytochemical localization of the receptor. Brain Res. *369:*316–320.

Altschuler, R.A., J.A. Juiz, S.E. Shore, S.C. Bledsoe, R.H. Helfert, and R.J. Wenthold (1993) Inhibitory amino acid synapses and pathways in the ventral cochlear nucleus. In M.A. Merchàn, J.A. Juiz, D.A. Godfrey, and E. Mugnaini (eds): The Mammalian Nuclei: Organization and Function. New York: Plenum, pp. 211–224.

Banay-Schwartz, M., Lajtha, A., and Palkovits, M. (1989) Changes with aging in the levels of amino acids in rat CNS structural elements. I. Glutamate and related amino acids. Neurochem. Res. *14:*555–562.

Berglund, A.M., and M.C. Brown (1994) Central trajectories of type II spiral ganglion cells from various cochlear regions in mice. Hear. Res. *75:*121–130.

Berrebi, A.S., and Mugnaini, E. (1991) Distribution and targets of the cartwheel cell axon in the dorsal cochlear nucleus of the guinea pig. Anat. Embryol. *183:*427–454.

Brown, M.C., A.M. Berglund, N.Y.S. Kiang, and D.K. Ryugo (1988) Central trajectories of type II spiral ganglion neurons. J. Comp. Neurol. *278:*581–590.

Caspary, D.M. (1986) Cochlear nuclei: Functional neuropharmacology of the principal cell types. In R.A. Altschuler, D.W. Hoffman, and R.P. Bobbin (eds): Neurobiology of Hearing: The Cochlea. New York: Raven, pp. 303–332.

Caspary, D.M., D.C. Havey, and C.L. Faingold (1979) Effects of microiontophoretically applied glycine and GABA on neuronal response patterns in the cochlear nuclei. Brain Res. *172:*179–185.

Caspary, D.M., L.P. Rybak, and C.L. Faingold (1985) The effects of inhibitory and excitatory amino acid neurotransmitters on the response properties of brainstem auditory neurons. In D. Drescher (ed): Auditory Biochemistry. Springfield: Thomas, pp. 198–226.

Caspary, D.M., K.E. Pazara, M. Kossl, and C.L. Faingold (1987) Strychnine alters the fusiform cell output from the dorsal cochlear nucleus. Brain Res. *417:*273–282.

Caspary, D.M., A. Raza, B.A. Lawhorn-Armour, J. Pippin, and S.P. Arneric (1990) Immunocytochemical and neurochemical evidence for age-related loss of GABA in the inferior colliculus: Implications for neural presbycusis. J. Neurosci. *10:*2363–2372.

Caspary, D.M., P.S. Palombi, P.M. Backoff, R.H. Helfert, and P.G. Finlayson (1993) GABA and glycine inputs control discharge rate within the excitatory response area of primary-like and phase-locked AVCN neurons. In M.A. Merchàn, J.A. Juiz, D.A. Godfrey, and E. Mugnaini (eds): The Mammalian Cochlear Nuclei: Organization and Function. New York: Plenum, pp. 239–252.

Caspary, D.M., P.M. Backoff, P.G. Finlayson, and P.S. Palombi (1994) Inhibitory inputs modulate discharge rate within frequency receptive fields of anteroventral cochlear nucleus neurons. J. Neurophysiol. *72:*2124–2133.

Caspary, D.M., J.C. Milbrandt, and R.H. Helfert (1995) Central auditory aging: GABA changes in the inferior colliculus. Exp. Gerontol. *30:*349–360.

Erway, L.C., J.F. Willott, J.R. Archer, and D. Harrison (1993) Genetics of age-related hearing loss in mice. I. Inbred and F1 hybrid strains. Hear. Res. *65:*125–132.

Feng, A.S., and M. Vater (1985) Functional organization of the cochlear nucleus of rufus horseshoe bats (*Rhinolophus rouxi*): Frequencies and internal connections are arranged in slabs. J. Comp. Neurol. *235:*529–553.

Godfrey, D.A., J.A. Carter, O.H. Lowry, and F.M. Matschinsky (1978) Distribution of gamma-aminobutyric acid, glycine, glutamate and aspartate in the cochlear nucleus of the rat. J. Histochem. Cytochem. *26:*118–126.

Henry, K.R., and R.A. Chole (1980) Genotypic differences in behavioral, physiological and anatomical expressions of age-related hearing loss in the laboratory mouse. Audiology *19:*369–383.

Hunter, K.P., and J.F. Willott (1987) Aging and the auditory brainstem response in mice with severe or minimal presbycusis. Hear. Res. *30:*207–218.

Kolston, J., K.K. Osen, C.M. Hackney, O.P. Otterson, and J. Storm-Mathisen (1992) An atlas of glycine- and GABA-like immunoreactivity and colocalization in the cochlear nuclear complex of the guinea pig. Anat. Embryol. *186:*443–465.

Lachica, E.A., L. Zirpel, and E.W. Rubel (1996) Intracellular mechanisms involved in the afferent regulation of neurons in the avian cochlar nucleus. In R.J. Salvi, D.H. Henderson, V. Colletti, and F. Fiorino (eds): Auditory Plasticity and Regeneration. New York: Thieme Medical Publishers, pp. 333–353.

Li, H.S. (1992) Genetic influences on susceptibility of the auditory system to aging and environmental factors. Scand Audiol. Suppl. *36:* 1–39.

Mikaelian, D.O. (1979) Development and degeneration of hearing in the C57/b16 mouse: Relation of electrophysiologic responses from the round window and cochlear nucleus to cochlear anatomy and behavioral responses. Laryngoscope *89:*1–15.

Milbrandt, J.C., and D.M. Caspary (1995) Age-related reduction of [^{3}H]strychnine binding sites in the cochlear nucleus of the Fischer 344 rat. Neuroscience *67:*713–719.

Milbrandt, J.C., R.L. Albin, and D.M. Caspary (1994) Age-related decrease in $GABA_B$ receptor binding in the Fischer 344 rat inferior colliculus. Neurobiol. Aging *15:*669–703.

Milbrandt, J.C., R.L. Albin, S.M. Turgeon, and D.M. Caspary (1996) $GABA_A$ receptor binding in the aging rat inferior colliculus. Neuroscience *73:*449–458.

Milbrandt, J.C., C. Hunter, and D.M. Caspary (1997) Alterations of $GABA_A$ receptor subunit mRNAs levels in the aged Fischer 344 rat inferior colliculus. J. Comp. Neurol. *379:* 455–465.

Mugnaini, E. (1985) GABA neurons in the superficial layers of the rat dorsal cochlear nucleus: Light and electron microscopic immunocytochemistry. J, Comp. Neurol. *235:*61–81.

Oertel, D., and R.E. Wickesberg (1993) Glycinergic inhibition in the cochlear nuclei: Evidence for tuberculoventral neurons being glycinergic. In M.A. Merchàn, J.A. Juiz, D.A. Godfrey, and E. Mugnaini (eds): The Mammalian Cochlear Nuclei: Organization and Function. New York: Plenum, pp. 225–238.

Osen, K.K., O.P. Ottersen, J. Storm-Mathisen (1990) Colocalization of glycine-like and GABA-like immunoreactivities: A semiquantitative study of individual neurons in the dorsal cochlear nucleus of cat. In O.P Ottersen and J. Storm-Mathisen (eds): Glycine Neurotransmission. New York: Wiley, pp. 417–451.

Palombi, P.S., and D.M. Caspary (1996a) Physiology of the aging Fisher 344 rat inferior colliculus: Responses to contralateral monaural stimuli. J. Neurophysiol. *76:*3114–3125.

Palombi, P.S., and D.M. Caspary (1996b) Responses of young and aged Fischer 344 rat inferior colliculus neurons to binaural tonal stimuli. Hear. Res. *100:*59–67.

Pan, H.S., K.A. Frey, A.B. Young, and J.B. Penney (1983) Changes in [^{3}H]muscimol binding in substantia nigra, entopeduncular nucleus, globus pallidus, and thalamus after striatal lesions as demonstrated by quantitative autoradiography. J. Neurosci. *3:*1189–1198.

Parham, K., and J.F. Willott (1988) The acoustic startle response in young and aging C57BL/6J and CBA/J mice. Behav. Neurosci. *102:*881–886.

Potashner, S.J., C.G. Benson, E.-M. Ostapoff, N. Lindberg, and D.K. Morest (1993) Glycine and GABA: Transmitter candidates of projections descending to the cochlear nucleus. In M.A. Merchàn, J.A. Juiz, D.A. Godfrey, and E. Mugnaini (eds): The Mammalian Cochlear Nuclei: Organization and Function. New York: Plenum, pp. 195–210.

Raza, A., J.C. Milbrandt, S.P. Arneric, and D.M. Caspary (1994) Age-related changes in brainstem auditory neurotransmitters: Measures of GABA and acetylcholine function. Hear. Res. *77:*221– 230.

Saint Marie, R.L., C.G. Benson, E.M. Ostapoff, and D.K. Morest (1991) Glycine immunoreactive projections from the dorsal to the anteroventral cochlear nucleus. Hear. Res. *51:*11–28.

Saint Marie, R.L., E.-M. Ostapoff, C.G. Benson, D.K. Morest, and S.J. Potashner (1993) Non-cochlear projections to the ventral cochlear nucleus: Are they mainly inhibitory? In M.A. Merchàn, J.A. Juiz, D.A. Godfrey, and E. Mugnaini (eds): The Mammalian Cochlear Nuclei: Organization and Function. New York: Plenum, pp. 121–131.

Saper, C.B. (1996) Any way you cut it: A new journal policy for the use of unbiased counting methods. J. Comp. Neurol. *364:*5.

Schwartz, I.R. (1981) The differential distribution of label following uptake of ^{3}H-labeled amino acids in the dorsal cochlear nucleus of the cat. Exp. Neurol. *73:*601–617.

Shone, G., R.A. Altschuler, J.M. Miller, and A.L. Nuttall (1991) The effect of noise exposure on the aging ear. Hear. Res. *56:*173–178.

Shore, S.E., R.H. Helfert, S.C. Bledsoe, R.A. Altschuler, and D.A. Godfrey (1991) Descending projections to the dorsal and ventral divisions of the cochlear nucleus in guinea pig. Hear. Res. *52:*255–268.

Wentold, R.J. (1987) Evidence for a glycinergic pathway connecting the two cochlear nuclei: An immunocytochemical and retrograde transport study. Brain Res. *415:*183–187.

Wenthold, R.J. (1991) Neurotransmitters of brainstem auditory nuclei. In R.A. Altschuler, D.W. Hoffman, and R.P. Bobbin (eds): Neurobiology of Hearing: The Cochlea. New York: Raven, pp. 121–139.

Wenthold, R.J., D. Huie, R.A. Altschuler, and K.A. Reeks (1987) Glycine immunoreactivity localized in the cochlear nucleus and superior olivary complex. Neuroscience *22:*897–912.

Wickesberg, R.E., and D. Oertel (1988) Tonotopic projection from the dorsal to the anteroventral cochlear nucleus of mice. J. Comp. Neurol. *268:*389–399.

Wickesberg, R.E., and D. Oertel (1990) Delayed, frequency specific inhibition in the cochlear nuclei of mice: A mechanism for monaural echo suppression. J. Neurosci. *10:*1762–1768.

Wickesberg, R.E., D. Whitlon, and D. Oertel (1994) In vitro modulation of somatic glycine-like immunoreactivity in presumed glycinergic neurons. J. Comp. Neurol. *339:*311–327.

Willott, J.F. (1986) Effects of aging, hearing loss, and anatomical location on thresholds of inferior colliculus neurons in C57BL/6 and CBA mice. J. Neurophysiol. *56:*391–408.

Willott, J.F. (1991) Aging and the Auditory System: Anatomy, Physiology, and Psychophysics. San Diego: Singular.

Willott, J. F. (1996) Auditory system plasticity in the adult C57BL/6J mouse. In R.J. Salvi, D.H. Henderson, V. Colletti, and F. Fiorino (eds): Auditory Plasticity and Regeneration. New York: Thieme Medical Publishers, pp. 297–316.

Willott, J.F., and S. Carlson (1995) Modification of the acoustic startle response in hearing-impaired C57BL/6J mice: Prepulse augmentation and prolongation of prepulse inhibition. Behav. Neurosci. *109:*396–403.

Willott, J.F., L.M. Jackson, and K.P. Hunter (1987) Morphometric study of the anteroventral cochlear nucleus of two mouse models of presbycusis. J. Comp. Neurol. *260:*472–480.

Willott, J.F., K. Parham, and K.P. Hunter (1988a) Response properties of inferior colliculus neurons in young and very old CBA/J mice. Hear. Res. *37:*1–14.

Willott, J.F., K. Parham, and K.P. Hunter (1988b) Response properties of inferior colliculus neurons in middle-aged C57BL/6J mice with presbycusis. Hear. Res. *37:*15–28.

Willott, J.F., L.S. Bross, and S.L. McFadden (1992) Morphology of the dorsal cochlear nucleus in young and aging C57BL/6J and CBA/J mice. J. Comp. Neurol. *321:*666–678.

Willott, J.F., L.S. Bross, and S.L. McFadden (1994) Morphology of the cochlear nucleus in CBA/J mice with chronic severe sensorineural cochlear pathology induced during adulthood. Hear. Res. *74:*1–21.

Willott, J.F., L.C. Erway, J.R. Archer, and D. Harrison (1995) Genetics of age-related hearing loss in mice. II. Strain differences and effects of caloric restriction on cochlear pathology and evoked response thresholds. Hear. Res. *88:*143– 155.

Winer, J.A., D.T. Larue, and G.D. Pollak (1995) GABA and glycine in the central auditory system of the mustache bat: Structural substrates for inhibitory neuronal organization. J. Comp. Neurol. *355:*355–317.

Wu, S.H., and D. Oertel (1986) Inhibitory circuitry in the ventral cochlear nucleus is probably mediated by glycine. J. Neurosci. *6:*2691–2706.

Young, E.D., I. Nelkin, and R.A. Conley (1995) Somatosensory effects on neurons in dorsal cochlear nucleus. J. Neurophysiol. *73:*743–765.

Zarbin, M.A., J.K. Wamsley, and M.J. Kuhar (1981) Glycine receptor: Light microscopic autoradiographic localization with [^{3}H]strychnine. J. Neurosci. *1:*532–547.

Zhang, S., and D. Oertel (1993) Tuberculoventral cells of the dorsal cochlear nucleus in mice: Intracellular recordings in slices. J. Neurophysiol. *69:*1409–1421.

Zhang, S., and D. Oertel (1994) Neuronal circuits associated with the output of the dorsal cochlear nucleus through fusiform cells. J. Neurophysiol. *71:*914–930.